Effect of Reactivity on Virtual Transition-State Structure for the Acylation Stage of Acetylcholinesterase-Catalyzed Hydrolysis of Aryl Esters and Anilides

Scott A. Acheson, Paul N. Barlow, Gerald C. Lee, Michael L. Swanson, and Daniel M. Quinn*

Contribution from the Department of Chemistry, The University of Iowa, Iowa City, Iowa 52242.
Received May 27, 1986

Abstract: The acylation stage of acetylcholinesterase-catalyzed hydrolysis of *p*-methoxyphenyl formate and of three anilides (*o*-nitrochloroacetanilide, *o*-nitroacetanilide, and *o*-nitroformanilide) has been studied by measuring substrate secondary and solvent isotope effects and by determining pL (L = H, D)-rate profiles and Eyring plots. The results of each of these probes support a model for acylation rate determination that involves a virtual transition state that contains contributions from the transition states of sequential physical and chemical steps. Eyring plots for all substrates are nonlinear and are interpreted in terms of temperature-dependent changes in fractional rate determination of sequential microscopic steps. For all substrates acylation reactivity increases sigmoidally with pH and depends on $pK_a^{H_2O}$ = 5.6–5.8, which is well below the intrinsic pK_a = 6.3 of the active site histidine. Solvent isotope effects for the anilide substrates are in the range 1.3–1.6. Proton inventory experiments indicate that intrinsic solvent isotope effects of ~2 that arise from general acid–base stabilization of the chemical transition state are partially masked by a solvent isotope-insensitive transition state that contributes 58–67% to acylation rate determination. For the most reactive substrate, *p*-methoxyphenyl formate, the solvent isotope effect is 1.09, which indicates that the solvent isotope-insensitive transition state is almost entirely rate determining. Substrate secondary deuterium kinetic isotope effects are consistent with decreasing nucleophilic interaction at the carbonyl carbon of the scissile bond of the substrate in the virtual acylation transition state with increasing k_{cat}/K_m. Hence, both solvent and substrate isotope effects indicate a general trend toward less acylation rate determination by chemical transition states as reactivity increases. The virtual transition-state model delineated herein lends quantitative support to Rosenberry's notion [Rosenberry, T. L. *Adv. Enzymol. Rel. Areas Mol. Biol.* **1975**, *43*, 103–218; *Proc. Natl. Acad. Sci. U.S.A.* **1975**, *72*, 3834–3838] that the acylation stage of acetylcholinesterase-catalyzed hydrolysis of neutral substrates is prominently rate limited by an induced fit conformation change that precedes chemical catalysis.

Considerable evidence has accumulated over the years that suggests a formal similarity between the mechanisms of serine protease[1-3] and acetylcholinesterase (AChE[4])[5,6] catalyses. Both catalyses involve nucleophilic attack by an active site serine on the carbonyl carbon of substrate and proceed via acylenzyme intermediates. Both catalyses are thought to involve stabilization of chemical transition states via general acid–base assistance by an active site histidine. Froede and Wilson[7] recently provided the first direct evidence for this mechanism when they demonstrated that 68% and 57% of AChE is in the acetylenzyme form during turnover of acetylcholine and acetylthiocholine, respectively.

Both acylation and deacylation stages of serine protease catalysis are thought to be rate limited by chemical steps that involve general acid–base transition-state stabilization. In contrast, Rosenberry[6,8] suggested that the acylation stage of AChE turnover of neutral substrates is prominently rate limited by an induced fit conformation change consequent to substrate binding. He based his model on the following observations: (a) Solvent isotope effects for V/K, which always monitors acylation,[9] are small (generally <1.5); (b) pK_a's determined from pH–rate profiles fall in the range 5.2–5.8[6,8,10,11] and are well below the pK_a ~ 6.3 of the active site histidine. Rosenberry's model predicts that the acylation transition state that is monitored by V/K is a virtual transition state[11-13] that is the weighted average of the transition state of a physical step (perhaps induced fit) and the transition state of the general acid–base step.

Quinn and Swanson[11] used a differential solvent isotope effect technique called the proton inventory method[14,15] to characterize the transition state for the acylation step of AChE-catalyzed hydrolysis of *o*-nitrochloroacetanilide (ONCA). The proton inventory for this reaction was quantitatively interpreted in terms of a virtual transition state that is comprised of a general acid–base transition state (29% rate limiting) and a solvent isotope and pH-insensitive transition state (71% rate limiting). In this paper we extend our quantitative analysis of acylation reaction dynamics and virtual transition-state structure to two additional anilide substrates, *o*-nitroformanilide (ONFA) and *o*-nitroacetanilide (ONA). Furthermore, solvent isotope effects and substrate isotope effects for four ester and anilide substrates that span a range of acylation reactivity of about 1000-fold are interpreted in terms of increasing exposure of chemical transition states with decreasing V/K.

* To whom correspondence should be addressed. This work was supported by NIH Grant NS21334. D.M.Q. is the recipient of a NIH Research Career Development Award (HL01583).

(1) Blow, D. M. *Acc. Chem. Res.* **1976**, *9*, 145–152.
(2) Stroud, R. M. *Sci. Am.* **1974**, *231*, 74–88.
(3) Hegazi, M. F.; Quinn, D. M.; Schowen, R. L. In *Transition States of Biochemical Processes*; Gandour, R. D., Schowen, R. L., Eds.; Plenum: New York, 1978; pp 355–428.
(4) Abbreviations: AChE, acetylcholinesterase; ONA, *o*-nitroacetanilide; ONCA, *o*-nitrochloroacetanilide; ONFA, *o*-nitroformanilide; PMPF, *p*-methoxyphenyl formate; $^{D}V/K$, secondary deuterium isotope effect for V/K; $^{D_2O}V/K$, solvent deuterium isotope effect for V/K; V/K, V_{max}/K_m; K_m, Michaelis constant; V, V_{max}; E, free enzyme, AChE; ES_1, Michaelis complex; ES_2, induced-fit complex; EA, acylenzyme; TLC, thin layer chromatography; L, H (hydrogen) or D (deuterium); pL, pH or pD; $[S]_0$ substrate concentration at reaction time 0; [S], substrate concentration; S, substrate; P, product; RB, round-bottomed; NMR, nuclear magnetic resonance; GC, gas chromatography; α-D effect, α-deuterium kinetic isotope effect; β-D effect, β-deuterium kinetic isotope effect; k_E, k_{cat}/K_m.
(5) Froede, J. S.; Wilson, I. B. In *The Enzymes*, 3rd ed.; Boyer, P. D., Ed.; Academic: New York, 1971; Vol 5, pp 87–114.
(6) Rosenberry, T. L. *Adv. Enzymol. Rel. Areas Mol. Biol.* **1975**, *43*, 103–218.
(7) Froede, H. C.; Wilson, E. B. *J. Biol. Chem.* **1984**, *259*, 11010–11013.
(8) Rosenberry, T. L. *Proc. Natl. Acad. Sci. U.S.A.* **1975**, *72*, 3834–3838.
(9) Reference 3, pp 376–378.
(10) Krupka, R. M. *Biochemistry* **1966**, *5*, 1983–1988.
(11) Quinn, D. M.; Swanson, M. L. *J. Am. Chem. Soc.* **1984**, *106*, 1883–1884.
(12) Schowen, R. L. In *Transition States of Biochemical Processes*; Gandour, R. D., Schowen, R. L., Eds.; Plenum: New York, 1978; pp 77–114.
(13) Stein, R. L. *J. Org. Chem.* **1981**, *46*, 3328–3330.
(14) Schowen, K. B. J. In *Transition States of Biochemical Processes*; Gandour, R. D., Schowen, R. L., Eds.; Plenum: New York, 1978; pp 225–283.
(15) Schowen, K. B.; Schowen, R. L. *Methods Enzymol.* **1982**, *87*, 551–606.

0002-7863/87/1509-0246$01.50/0

Experimental Section

Materials. Acetylcholinesterase (EC 3.1.1.7) from electric eel was obtained from Sigma Chemical Co. as a lypophilized powder. Prior to use the enzyme was dissolved in 0.1 M sodium phosphate buffer, pH 7.3, that contained 0.1 N NaCl. The buffered enzyme was stored frozen at −20 °C and was stable for over a month. $(CD_3CO)_2O$ (>99% D), *p*-methoxyphenol, and acetyl chloride were purchased from Sigma Chemical Co. and used as obtained. DCO_2Na (>99% D) and $ClCD_2CO_2D$ (>98% D) were purchased from MSD Isotopes. The latter compound was vacuum sublimed before use. Deuterium oxide (99.8% D) was purchased from Aldrich Chemical Co. and was used as received. Water used for buffer preparations was distilled. Buffer components (sodium citrate, citric acid, sodium phosphates) were reagent grade chemicals. Buffers used for enzyme kinetics were sterilized by filtration through 0.45 μm Millex HA filters (Millipore Corp.). Anhydrous diethyl ether was purchased from Mallinckrodt and $SOCl_2$ from Matheson, Coleman and Bell. Chloroacetyl chloride, *o*-nitroaniline, and spectrophotometric grade gold-label CH_3CN were from Aldrich Chemical Co.

Synthesis and Characterization of Substrates. The isotopic ONFAs,[16] $o\text{-}O_2NC_6H_4NHCOL$, and the isotopic PMPFs,[17] $p\text{-}MeOC_6H_4OCOL$, were synthesized by the mixed acetic–formic anhydride method. In a typical synthesis, 2 g (0.023 mol) of CH_3CO_2COL, which was synthesized from CH_3COCl and LCO_2Na by the method of Fieser and Fieser,[18] were dissolved in 5 mL of anhydrous diethyl ether in an ice-cooled RB flask. Either *o*-nitroaniline or *p*-methoxyphenol (0.023 mol) dissolved in 50 mL of anhydrous diethyl ether was added dropwise with stirring to the RB flask. For synthesis of PMPFs a few drops of pyridine were added to catalyze the reaction. The reaction mixture was stirred overnight, and the ether was removed by rotoevaporation. The crude formanilides were twice recrystallized from 95% EtOH to yield yellow crystals that melted at 123–124 °C (lit.[19] mp 122 °C). Proton NMR and mass spectra are consistent with the expected structures of the isotopic ONFAs and with an isotopic purity >95% for the formyl-D compound. The crude formates were lyophilized for 1–2 h to remove acetic acid and were purified by column chromatography on silica gel (J.T. Baker Chemical Co., 60–200 mesh). The purified protio formate melted at 30–31 °C, and the purified deuterio formate at 33–34 °C (lit.[17] mp 32–33 °C). Proton NMR and mass spectra are consistent with the expected structures of the isotopic PMPFs and with an isotopic purity >98% for the formyl-D ester. The isotopic ONFAs and PMPFs gave single spots when analyzed by TLC on precoated plastic slides (Macherey-Nagel) with CH_2Cl_2 or 0.4% (v/v) glacial acetic acid in $CHCl_3$ as the respective mobile phases.

The isotopic ONCAs, $o\text{-}O_2NC_6H_4NHCOCL_2Cl$, were synthesized by adding 1.15 mL (0.0144 mol) of the respective chloroacetyl chloride in 10 mL of benzene dropwise and with stirring to an ice-cooled RB flask that contained 2.0 g of *o*-nitroaniline (0.0144 mol) and 2.5 mL (0.02 mol) dimethylaniline in 200 mL of benzene. The rate of addition was such that the reaction temperature never exceeded 10 °C. The mixture was stirred overnight, and the dimethylanilinium hydrochloride precipitate was removed by filtration. The precipitate was washed with benzene, and the wash solvent was combined with the reaction solvent and rotoevaporated. The resulting yellow oil was recrystallized from MeOH to produce yellow needles: mp 87 °C, protio anilide; mp 86–87.5 °C, deuterio anilide; lit.[20] mp 88 °C. The isotopic ONCAs gave single spots with identical R_f 0.6 on precoated TLC slides in the solvent system petroleum ether: propionic acid (11:4 (v/v)). Proton NMR and mass spectra are consistent with the expected structures of the anilides. The isotopic purity of the deuterated anilide was estimated at 93% by NMR. Deuterated chloroacetyl chloride, $ClCD_2COCl$, was prepared by refluxing overnight 2 g (0.021 mol) of $ClCD_2CO_2D$ and 1.7 mL (0.024 mol) of glass distilled $SOCl_2$.[21] The acid chloride was isolated by simple distillation and used immediately for the synthesis of deuterated ONCA.

The isotopic ONAs, $o\text{-}O_2NC_6H_4NHCOCL_3$, were prepared by the method of Fieser and Martin.[22] To a solution of 3.45 g (0.025 mol) of *o*-nitroaniline in 25 mL of benzene in an RB flask at room temperature was added, with stirring, 3.47 g of acetic anhydride and 2–3 drops of concentrated H_2SO_4. The solution was warmed gently for 30 min, and the solvent was removed by rotoevaporation. The resulting yellow solid was recrystallized from EtOH:H_2O (3:1 (v/v)). For synthesis of the deuterio ONA 2.0 g of $(CD_3CO)_2O$ were used and the amounts of the other reaction components were scaled accordingly. Both isotopic anilides melted at 92–93 °C (lit.[22] mp 92–93 °C). The respective anilides gave single spots on precoated TLC slides with CH_2Cl_2 as the mobile phase. Proton NMR and mass spectra are consistent with the expected structures of the anilides and with an isotopic purity >99% for deuterio ONA.

Proton spectra were obtained on JEOL FX90Q or Perkin-Elmer R12 NMR spectrometers. Mass spectra were obtained on a Hewlett-Packard 5985 GC–mass spectrometer that was operated in the electron ionization mode at 70 eV.

Enzyme Kinetics and Data Reduction. For the measurement of solvent isotope effects, buffers of equivalent pL were utilized. Equivalent buffers in H_2O and D_2O are those for which the concentrations of buffer components and NaCl (or other salts) are the same.[14,15] A Corning Model 125 pH meter equipped with a glass combination electrode was used for the measurement of buffer pH's. For D_2O buffers, pD's were determined by adding 0.4 pH units to the pH meter reading.[14,15,23] Stock substrate solutions were prepared in CH_3CN, and hence each kinetic run contains a low percentage of this solvent. Nonetheless, $^{D_2O}V/K$ (=1.57 ± 0.06, measured by initial rates) for ONA hydrolysis did not change as the volume percent of CH_3CN was varied from 0.5% to 4.0%.

Timecourses for the hydrolysis of *o*-nitroanilides were followed at 413 nm and for the hydrolysis of PMPF at 287 nm or 306 nm with a Beckman DU7 UV–vis spectrophotometer that is interfaced to an IBM Personal Computer. Reactions were done in 1 cm path length, 1.4 mL capacity, self-masking cuvettes in the water-jacketted cell holder of the DU7. Reaction temperature was controlled (±0.05 °C) by using a VWR 1140 refrigerated, circulating water bath. Initial rates were determined by linear-least-squares analysis of timecourses that comprised <5% of total substrate turnover. First-order rate constants (V/K) were measured by using $[S]_0 < 0.1K$ and calculated by nonlinear-least-squares fitting of timecourse data to eq 1. A, A_0, and A_∞ are the absorbances at times

$$A = (A_0 - A_\infty)e^{-kt} + A_\infty \quad (1)$$

t, 0, and ∞, respectively; k is the first-order rate constant. Reactions were followed for at least 3 half-lives. For ester hydrolyses V and V/K were sometimes determined by nonlinear-least-squares fitting of timecourse data to the integrated form of the Michaelis–Menten equation:

$$t = \frac{K}{V}\ln\frac{A_0 - A_\infty}{A - A_\infty} + \frac{1}{V\Delta\epsilon}(A_0 - A) \quad (2)$$

Equation 2 is the integrated Michaelis–Menten equation in terms of absorbance, and it was derived from the integrated equation in terms of [S] by using eq 3. Equations 3 only hold for irreversible reactions. In

$$[S] = \frac{A - A_\infty}{\Delta\epsilon} \qquad [S]_0 = \frac{A_0 - A_\infty}{\Delta\epsilon} \quad (3)$$

eq 2 and 3, $\Delta\epsilon = \epsilon_s - \epsilon_p$, where ϵ_s and ϵ_p are the absorptivity constants of S and P, respectively.

pL–rate profile data were fit by nonlinear least squares to eq 4. In

$$k = \frac{k_{lim}K_a}{[H^+] + K_a} \quad (4)$$

eq 4, k is the first-order rate constant or initial velocity, k_{lim} is the limiting or maximal rate constant at high pH, and K_a is the apparent acid ionization constant for an AChE amino acid side chain whose conjugate base is necessary for enzyme activity.

Nonlinear-least-squares analysis of proton inventory data and Eyring plots are described in the Results section.

Results

pL–Rate Profiles. The dependences of V/K on pH and pD were determined for AChE-catalyzed hydrolysis on ONFA (Figure 1A), of ONA (Figure 1B), and of PMPF. The sigmoidal fits in Figure 1 are nonlinear-least-squares fits to eq 4 (cf. Experimental Methods). The results of these analyses and the corresponding solvent isotope effects for V/K are gathered in Table I and are compared to the values reported by Quinn and Swanson[11] for AChE-catalyzed hydrolysis of ONCA. The ΔpK_a's for ONA, ONFA, and PMPF are noteworthy since they are larger than ΔpK_a's of 0.45–0.55 for various weak acids.[15] The pK_a's of imidazole in L_2O that contains 0.1 N NaCl yield $\Delta pK_a = 0.49$,[24]

(16) Hurd, C. D.; Roe, A. S. *J. Am. Chem. Soc.* **1939**, *61*, 3355–3359.
(17) Stevens, W.; Van Es, A. *Recl. Trav. Chim. Pays-Bas* **1965**, *84*, 1247–1252.
(18) Fieser, M.; Fieser, L. *Reagents for Organic Synthesis*; Wiley: New York, 1969; Vol 2, pp 10–12.
(19) *Beilsteins's Handbuch Der Organischen Chemie*, 4th ed.; Prager, B., Jacobson, P., Schmidt, P., Stern, D., Eds.; Springer-Verlag: Berlin, 1929; Vol 12, p 691.
(20) *Beilstein's Handbuch Der Organischen Chemie*, 4th ed.; Richter, F., Ed.; Springer-Verlag: Berlin, 1933; Vol 12, Suppl. 1, p 342.
(21) Gerrard, W.; Thrush, A. M. *J. Chem. Soc.* **1953**, 2117–2120.
(22) Fieser, L. F.; Martin, E. L. *J. Am. Chem. Soc.* **1935**, *57*, 1835–1839.
(23) Salomaa, P.; Schaleger, L. L.; Long, F. A. *J. Am. Chem. Soc.* **1964**, *86*, 1–7.

Table I. Solvent Isotope Effects for Various Acetylcholinesterase-Catalyzed Reactions

substrate	rel k_E[a]	$^{D_2O}V/K$	$pK_a^{H_2O}$	$pK_a^{D_2O}$
ONFA[b]	1	1.41 ± 0.03	5.62 ± 0.04	6.23 ± 0.03
ONA[c]	4	1.55 ± 0.03	5.63 ± 0.03	6.44 ± 0.04
ONCA[d]	53	1.31 ± 0.02	5.80 ± 0.03	6.19 ± 0.03
PMPF[e]	1595	1.09 ± 0.01	5.62 ± 0.10	6.19 ± 0.05

[a] Except where indicated, all kinetic runs were done at 25.00 ± 0.05 °C in 1.00 mL buffer. For PMPF, $k_E = 3.1 \times 10^6$ M^{-1} s^{-1} and K = 2.02 mM at pH 7.24 in 0.1 M sodium phosphate buffer that contained 0.1 N NaCl and 2% MeCN (v/v). The active site concentration of AChE samples was determined by fluorescent titration with *N*-methyl(7-dimethylcarbamoxy)quinolinium iodide, as described by Rosenberry and Bernhard.[45] Error limits of isotope effects were calculated as described in footnote *b* of Table III. [b] K = 2.1 mM at pH 7.24 and 25 °C. pK_a's were calculated from the pL–rate profiles of Figure 1. The solvent isotope effect for V/K is the ratio of limiting velocities at high pL calculated from the pL–rate profiles of Figure 1. [c] K = 20 mM at pH 7.24 and 25 °C. Solvent isotope effects and pK_a's were determined as described in footnote *b*. [d] K = 0.8 mM at pH 7.24 and 25 °C. The solvent isotope effect for V/K was calculated from slopes of Lineweaver–Burk plots constructed from initial velocities measured in 0.1 M sodium phosphate buffer, pH 7.24, that contained 0.1 N NaCl and 2% CH_3CN (*v*/*v*). pK_a's were calculated from the pL–rate profiles of Quinn and Swanson.[11] [e] The solvent isotope effect for V/K and pK_a's were determined from pL–rate profiles. V/K was determined by fitting timecourse data to the integrated Michaelis–Menten equation (eq 2 of Experimental Section). Reactions were conducted at 20.00 ± 0.05 °C in 1.00 mL of buffer that contained 0.1 N NaCl, 2% CH_3CN (v/v), and 13 nM AChE.

which falls in the cited range,[15] and $\Delta pK_a = 0.50 \pm 0.06$ for V of ACHE-catalyzed hydrolysis of *o*-nitrophenyl acetate (a reaction that is entirely rate limited by proton transfer transition states).[24] Hence, the large ΔpK_a's calculated herein from pL–rate profiles are likely not due to the intrinsic ionization behavior of the imidazole functionality of the AChE active site histidine. Moreover, the pK_a's in H_2O are well below the suspected intrinsic $pK_a \sim 6.3$ of the active site histidine.[6,8] Both the large ΔpK_a's and the low pK_a's in H_2O can be rationalized in terms of a virtual transition state (cf. Discussion).

Proton Inventories. The theory of application of the proton inventory technique to enzyme reactions has been thoroughly described.[14,15] The general expression for the dependence of enzymic rate or rate constant on the atom fraction n of deuterium in the solvent is given by the Gross–Butler equation:

$$k_n = k^{H_2O}\frac{\prod_j(1 - n + n\Phi_j^T)}{\prod_i(1 - n + n\Phi_i^R)} \quad (5)$$

The Gross–Butler equation contains a product of terms in the numerator for each of j transition state protons that contribute to the solvent isotope effect. The contribution of each transition state proton is the reciprocal of the respective fractionation factor, Φ_j^T. Only protons that have fractionation factors different than unity contribute to the solvent isotope effect. One can generally expect transition-state protonic interactions to contribute to the solvent isotope effect if the protons are involved in general acid–base bridges.[14,15] The denominator of eq 5 contains a product of terms for reactant-state protons. Since the rapidly exchanging protons of common amino acid functionalities have $\Phi_i^R \sim 1$,[14,15,25] the Gross–Butler equation reduces to a polynomial function of n that contains only transition-state terms. Hence, if a single transition-state protonic interaction (e.g., a general acid–base proton bridge) contributes to the solvent isotope effect, the observed rate constant will vary linearly with n. If two or more transition-state protonic interactions contribute to the solvent isotope effect, the plot will be nonlinear and downward bulging.[14,15]

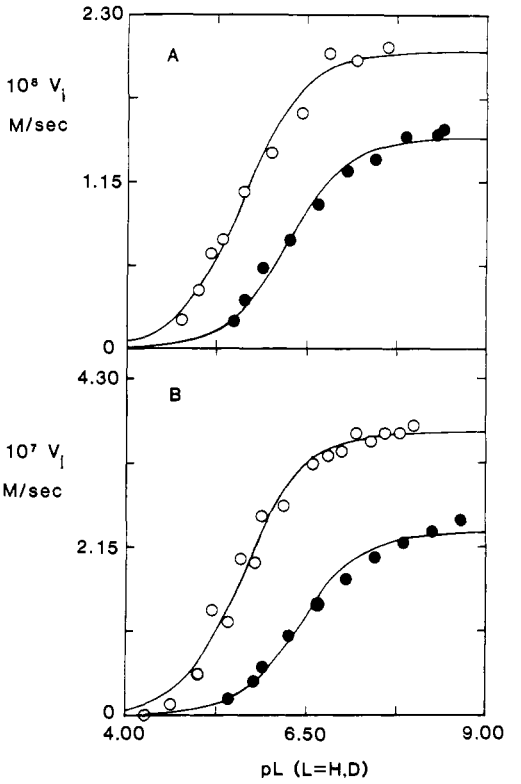

Figure 1. pL–rate profiles (L = H, D) for initial velocities of AChE-catalyzed hydrolyses of ONFA and ONA. Reactions were conducted at 25.00 ± 0.05 °C in 1.00 mL of 0.1 M sodium citrate/citric acid buffer (pH < 5.60 and pD < 6.25) or 0.1 M sodium phosphate buffer that contained 0.1 N NaCl. Velocities in H_2O are denoted by open circles and those in D_2O by closed circles. (A) Reactions contained 0.1 mM ONFA (=0.05K), 2% MeCN (v/v), and 49 nM AChE. (B) Reactions contained 0.1 mM ONA (=0.005K), 0.4% MeCN (v/v), and 114 nM AChE.

Because of the dependence of the shape of the plot on the number of transition-state protons that contribute solvent isotope effects, the proton inventory method has been used to distinguish simple general acid–base catalysis from multifunctional (multiproton) catalysis for serine protease[26–30] and amidohydrolase[31] action.

Figure 2 shows proton inventory plots for V/K of AChE-catalyzed hydrolysis of ONFA and ONA. The shape of the plots is nonlinear and upward bulging and hence corresponds to none of the situations discussed in the last paragraph. A similar proton inventory was reported by Quinn and Swanson[11] for the acylation stage (monitored by V/K) of AChE-catalyzed hydrolysis of ONCA. The ONCA proton inventory was interpreted in terms of a virtual transition state that consists of contributions from the transition state for a partially rate-determining general acid–base chemical step and that for a partially rate-determining physical step that is solvent isotope insensitive and pH insensitive. Hence, the bulging upward shape of the proton inventories of Figure 2 and that of Quinn and Swanson[11] signals a change in rate-determining step as H_2O is replaced by D_2O. As will be delineated in the Discussion section, this model quantitatively accommodates the nonlinear proton inventories of Figure 2 and explains why the

(24) Acheson, S. A.; Dedopoulou, D.; Quinn, D. M. *J. Am. Chem. Soc.*, preceding paper in this issue.
(25) Jarret, R. M.; Saunders, M. *J. Am. Chem. Soc.* **1985**, *107*, 2648–2654.
(26) Hunkapiller, M. W.; Forgac, M. D.; Richards, J. H. *Biochemistry* **1976**, *15*, 5581–5588.
(27) (a) Pollack, E.; Hogg, J. L.; Schowen, R. L. *J. Am. Chem. Soc.* **1973**, *95*, 969. (b) Quinn, D. M.; Elrod, J. P.; Ardis, R.; Friesen, P.; Schowen, R. L. *J. Am. Chem. Soc.* **1980**, *102*, 5358–5365.
(28) Elrod, J. P.; Hogg, J. L.; Quinn, D. M.; Venkatasubban, K. S.; Schowen, R. L. *J. Am. Chem. Soc.* **1980**, *102*, 3917–3922.
(29) Stein, R. L.; Elrod, J. P.; Schowen, R. L. *J. Am. Chem. Soc.* **1983**, *105*, 2446–2552.
(30) (a) Stein, R. L. *J. Am. Chem. Soc.* **1983**, *105*, 5111–5116. (b) Stein, R. L. *J. Am. Chem. Soc.* **1985**, *107*, 5767–5775.
(31) Quinn, D. M.; Venkatasubban, K. S.; Kise, M.; Schowen, R. L. *J. Am. Chem. Soc.* **1980**, *102*, 5365–5369.

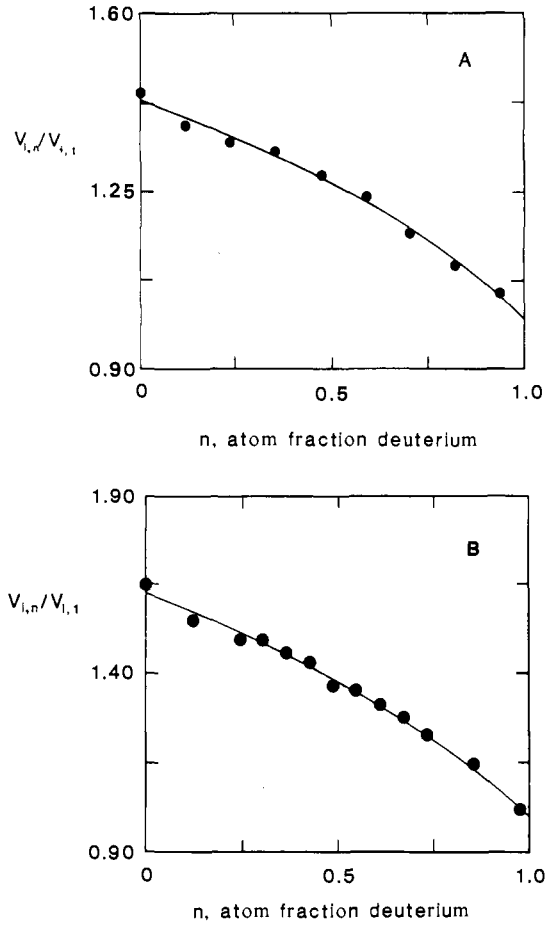

Figure 2. Proton inventories for AChE-catalyzed hydrolyses of ONFA and ONA. Reactions were conducted at 25.00 ± 0.05 °C in 1.00 mL of 0.1 M sodium phosphate buffer, pH 7.30 and equivalent pL,[14,15] that contained 0.1 N NaCl and 0.34 μM AChE. First-order rate constants (V/K's) were calculated by nonlinear-least-squares fitting of timecourse data to eq 1 of the Experimental Section. Curvilinear fits of proton inventories are nonlinear-least-squares fits to eq 13 of the Discussion. (A) ONFA proton inventory; $[ONFA]_0$ = 0.1 mM (=0.05K). Reactions also contained 2% MeCN (v/v). (B) ONA proton inventory; $[ONA]_0$ = 0.5 mM (=0.025K).

pK_a's determined from the pH–rate profiles of Figure 1 are well below the suspected intrinsic pK_a ~ 6.3 of the active site histidine.[6,8]

Hogg et al.[32] reported a bulging upward proton inventory for the acylation stage of AChE-catalyzed hydrolysis of *p*-nitrophenyl acetate. However, they interpreted their data in terms of an inverse isotope effect contribution of 1.4 from an enzyme reactant state proton that partially offsets an isotope effect of 2.2 from a general acid–base transition-state proton bridge.

Temperature Dependence of V/K. The temperature dependences of V/K for AChE-catalyzed hydrolyses of ONFA, ONA, ONCA, and PMPF have been determined over the range 12–40 °C. The Eyring plots[33] for all four substrates are curvilinear downward, as the plot for PMPF illustrates in Figure 3. This type of temperature dependence has two possible explanations: (a) The plot curves downward because the enzyme is less stable at higher temperatures. This explanation is unlikely because the Eyring plot for V of AChE-catalyzed hydrolysis of PMPF is linear (cf. Figure 3) in both H_2O and D_2O. (b) The contributions of individual microscopic steps to rate determination are changing with temperature. This explanation is consistent with the assignment of a virtual transition state for the acylation step. The

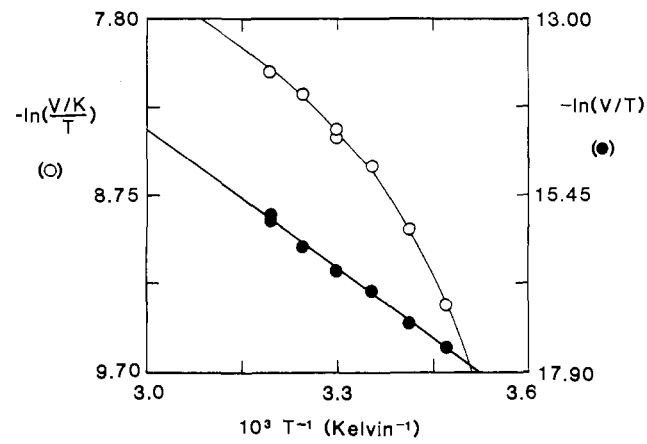

Figure 3. Eyring plots for V/K (open circles) and V (closed circles) of AChE-catalyzed hydrolysis of PMPF. Reactions were conducted in 1.00 mL of 0.1 M sodium phosphate buffer, pH 6.97, that contained 0.1 N NaCl, 2% MeCN (v/v), $[PMPF]_0$ = 2 mM, and 13 nM AChE. The curvilinear fit of the V/K plot is a nonlinear-least-squares fit to eq 7 of Results.

increasing expression of a solvent isotope effect for V/K of PMPF hydrolysis with decreasing temperature supports this model. At pH 6.90 and pD 7.47 the isotope effects were $^{D_2O}V/K$ = 1.02 ± 0.03 at 35 °C and $^{D_2O}V/K$ = 1.20 ± 0.08 at 15 °C.

The simplest mechanism that can accommodate the shape of the Eyring plots involves two serial microscopic steps that contribute to acylation rate determination. In this case, the observed acylation rate constant is the harmonic mean of the overall rate constants for passage of free E and S over each of the partially rate-determining transition states:

$$1/k_E = 1/k_2' + 1/k_3' \qquad (6)$$

In eq 6, $k_E = k_{cat}/K_m$ and k_2' and k_3' are overall rate constants for acylation events that follow formation of the Michaelis complex. A more complete delineation of the derivation of eq 6 is saved for the Discussion.

The Eyring equation that corresponds to eq 6 follows:

$$\ln \frac{k_E}{T} = -\ln (A_2 e^{\Delta H^{\ddagger}_2/RT} + A_3 e^{\Delta H^{\ddagger}_3/RT}) \qquad (7)$$

In eq 7 $A = (h/k_B)e^{-\Delta S^{\ddagger}/R}$, where h and k_B are Planck's and Boltzman's constants, respectively. The curvilinear fit of Figure 3 is a calculated nonlinear-least-squares fit to eq 7. The fit was performed by calculating a four-dimensional grid of combinations of the parameters A_2, A_3, $\Delta H^{\ddagger}_2$, and $\Delta H^{\ddagger}_3$ and by searching the grid for the combination that gives the minimum sum of squared residuals. Error limits of the parameters were calculated by repeating the grid search ten times with random noise added to each ln (k_E/T). The average reproducibility of observed ln (k_E/T) was used as an estimate of the random noise. The standard deviation of the mean for each of the parameters was calculated from the values calculated in the ten grid searches. This computational procedure yielded the values for $\Delta S^{\ddagger}$ and $\Delta H^{\ddagger}$ that are given in Table II.

Secondary Isotope Effects. Secondary deuterium kinetic isotope effects for V/K have been measured for ONA, ONFA, ONCA, and PMPF and are given in Table III. Inverse α-D and β-D effects were observed for the two least reactive substrates, ONFA and ONA. The secondary isotope effects for the most reactive substrates, PMPF and ONCA, are within experimental error of unity.

Discussion

Rosenberry[6,8] noted that for good acetate ester substrates the acylation stage of AChE catalysis was subject to small solvent isotope effects and pH–rate profile pK_a's that were ~5.5, which are well below the pK_a = 6.3 of the active site histidine. He inferred from these results that for good substrates the acylation stage is prominently rate limited by a nonchemical event that is

(32) Hogg, J. L.; Elrod, J. P.; Schowen, R. L. *J. Am. Chem. Soc.* **1980**, *102*, 2082–2086.
(33) Glasstone, S.; Laidler, K. J.; Eyring, H. *The Theory of Rate Processes*; McGraw-Hill: New York, 1941.

Table II. Activation Parameters for Acetylcholinesterase-Catalyzed Reactions[a]

substrate	solvent	$\Delta H^{\ddagger}_2$	$\Delta S^{\ddagger}_2$	$\Delta H^{\ddagger}_3$	$\Delta S^{\ddagger}_3$
ONFA[b]	H_2O	0.2 ± 0.1	−70.4 ± 0.1	9.9 ± 0.1	−39.6 ± 0.3
	D_2O	0.7 ± 0.3	−69.9 ± 0.7	10.0 ± 0.2	−39.7 ± 0.6
ONA[c]	H_2O	1.5 ± 0.5	−64 ± 1	13 ± 2	−24 ± 4
	D_2O	4 ± 1	−57 ± 3	15 ± 3	−17 ± 11
ONCA[c]	H_2O	0.0 ± 0.4	−65.6 ± 0.8	10.0 ± 0.5	−32.0 ± 0.5
	D_2O	−1.3 ± 0.7	−71 ± 2	9.7 ± 0.7	−33 ± 2
PMPF[d]	H_2O	3.8 ± 0.2	−45.5 ± 0.6	24.1 ± 0.3	24.4 ± 0.7
	D_2O	4.2 ± 0.7	−44 ± 2	24.6 ± 0.6	26 ± 2

[a] Activation parameters were calculated by nonlinear-least-squares fits of Eyring plot data to eq 7, as described in the Results. Values for ONA, ONCA, and PMPF are means calculated from two Eyring plots. Values for ONFA are calculated from single Eyring plots. Units are kcal mol^{-1} and cal K^{-1} mol^{-1} for activation enthalpies and entropies, respectively. [b] Eyring plots were constructed from initial velocities measured at $[S]_0 \ll K$ in 0.1 M sodium phosphate buffer, pH 7.30 or pD 7.85, that contained 0.1 N NaCl, 2% MeCN (v/v), and 49 nM AChE. [c] Eyring plots were constructed from first-order rate constants (V/K's) calculated by fitting timecourse data to eq 1 of the Experimental Section. Experimental conditions were as described in footnote *b*, except that ONA reactions contained 0.14 μm AChE and ONCA reactions contained 39 or 64 nM AChE. [d] Eyring plots were constructed from V/K's that were calculated by fitting timecourse data to the integrated Michaelis–Menten equation (eq 2 of Experimental Section). Reactions were run in 0.1 M sodium phosphate buffer, pH 6.90 or pD 7.47, that contained 0.1 N NaCl, 2% MeCN (v/v), and 13 nM AChE.

Table III. Kinetic Secondary Deuterium Isotope Effects for AChE-Catalyzed Reactions

substrate	isotopic substitution	N^a	$^{D}V/K^b$
ONFA[c]	α-L	16 H, 15 D	0.88 ± 0.02
ONA[d]	β-L3	4 H, 4 D	0.982 ± 0.005
ONCA[e]	β-L2	4 H, 4 D	1.02 ± 0.02
PMPF[f]	α-L	13 H, 12 D	0.99 ± 0.01

[a] N is the number of kinetic runs with each isotopic substrate. Reactions were conducted at 25.00 ± 0.05 °C in 0.1 M sodium phosphate buffer that contained 0.1 N NaCl and 2% MeCN (v/v). [b] Isotope effects are the ratios of first-order rate constants that were calculated by nonlinear-least-squares fitting of timecourse data to eq 1 of the Experimental Section. Error limits of isotope effects were calculated by the following equation: $\Delta^{D}k = {}^{D}k[(\Delta k_H/k_H)^2 + (\Delta k_D/k_D)^2]^{1/2}$. [c] ONFA reactions were conducted at pH 7.30 and contained 0.29, 0.34, or 0.57 μM AChE. [d] ONA reactions were conducted at pH 7.30 and contained 0.14 μM AChE. [e] ONCA reactions were conducted at pH 7.30 and contained 38 nM AChE. The isotope effect is the same at 15 °C. [f] PMPF reactions were conducted at pH 6.08 and contained 2.5, 5.1, or 6.4 nM AChE.

pH and solvent isotope insensitive. The proton inventory experiments and pL–rate effects described by Quinn and Swanson[11] and by Acheson et al.[24] provide quantitative support for Rosenberry's general model for AChE acylation reaction dynamics.

In this paper we describe the effects of temperature, pH, and solvent deuterium and substrate isotopic substitution on V/K for AChE-catalyzed hydrolysis of three anilides and an ester. This set of substrates was chosen because its constituents are closely isosteric yet span a range of acylation reactivity of over three orders of magnitude. We rationalized that it may be possible to effect increasing exposure to rate determination of chemical transition states by using a set of structurally similar substrates whose members span a wide acylation reactivity range. The secondary isotope effects of Table III show that this expectation is correct. For the least reactive substrate, ONFA, the α-D effect is roughly 40% that expected for full sp^2 to sp^3 rehybridization on conversion of the E + S reactant state to a tetrahedral intermediate that precedes the acylenzyme (Scheme I).

The α-D effect of 0.88 ± 0.02 for the ONFA reaction is consistent with either of the following mechanistic models: (a) The observed α-D effect is the intrinsic effect arising from an acylation transition state(s) wherein the bond order between the carbonyl carbon and the active site serine or the anilide leaving group is around 0.4. (b) Acylation is rate limited by a virtual transition state for which the intrinsic α-D effect is masked by partial rate

Scheme I

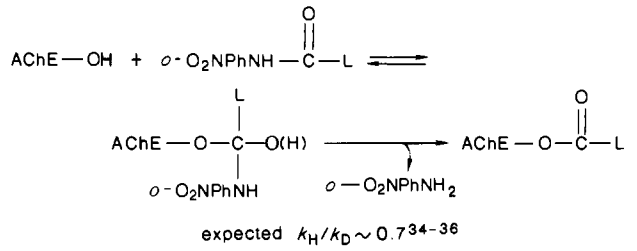

Scheme II

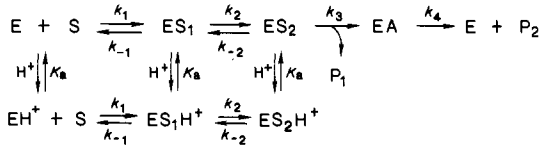

determination by a transition state that does not involve nucleophilic AChE–substrate interaction. The latter interpretation is favored because as the acylation reactivity of the substrate increases the corresponding secondary isotope effect approaches unity (cf. Table III). For example, the β-D effect for V/K of ONA hydrolysis is 0.6 ± 0.2% per D, which is about 15% of the expected β-D effect for full sp^2 to sp^3 rehybridization of the substrate carbonyl carbon.[34-37] For the most reactive substrates, ONCA and PMPF, the corresponding β-D and α-D effects are within experimental error of unity, which is consistent with little or no rehybridization in the respective acylation transition states. The trend toward less transition state sp^2 to sp^3 rehybridization with increasing reactivity could be due to a highly plastic AChE active site that can accommodate high transition state structure variability. However, the solvent isotope effects for V/K of Table I also support a trend toward decreasing contribution of chemical transition states to acylation rate determination as reactivity increases.

Scheme II outlines a kinetic mechanism for AChE catalysis that can accommodate the diverse observations reported herein. The crux of this acylation mechanism is that two kinetically significant steps, k_2 and k_3, follow formation of ES_1. This mechanism is identical with that proposed by Rosenberry[6,8] and includes the simplifying assumption that the protonic equilibria are the same for the species involved in the acylation stage of catalysis. A steady-state derivation gives the following expression for k_E:

$$k_E = \frac{k_1k_2k_3}{k_{-1}\left[k_{-2}\left(1 + \frac{[H^+]}{K_a}\right) + k_3\right]} \quad (8)$$

Equation 8 is also based on the assumption that the binding step k_1 does not contribute significantly to rate determination for k_E.[38]

(34) (a) Hogg, J. L.; Rodgers, J.; Kovach, I.; Schowen, R. L. *J. Am. Chem. Soc.* **1980**, *102*, 79–85. (b) Kovach, I. M.; Hogg, J. L.; Raben, T.; Halbert, K.; Rodgers, J.; Schowen, R. L. *J. Am. Chem. Soc.* **1980**, *102*, 1991–1999. (c) Hogg, J. L. In *Transition States of Biochemical Processes*; Gandour, R. D., Schowen, R. L., Eds.; Plenum: New York, 1978; pp 201–224.

(35) Kirsch, J. F. In *Isotope Effects on Enzyme-Catalyzed Reactions*; Cleland, W. W., O'Leary, M. H., Northrop, D. B., Eds.; University Park Press: Baltimore, 1977; pp 100–121.

(36) Klinman, J. P. *Adv. Enzymol. Rel. Areas Mol. Biol.* **1978**, *46*, 415–494.

(37) Kovach, I. M.; Belz, M.; Larson, M.; Rousy, S.; Schowen, R. L. *J. Am. Chem. Soc.* **1985**, *107*, 7360–7365.

(38) For highly reactive ester substrates binding may contribute to rate determination. In this case k_E is

$$k_E = \frac{k_1k_2k_3}{k_{-1}\left[k_{-2}\left(1 + \frac{[H^+]}{K_a}\right) + k_3\right] + k_3k_2}$$

This equation reduces to eq 8 of the text when $k_{-1}k_3 \gg k_2k_3$, i.e., when binding does not contribute to rate determination.

This assumption is reasonable for the anilide substrates ONFA, ONA, and ONCA, which have k_E's that are one to four orders of magnitude smaller than those of closely isosteric aryl ester substrates (cf. ref 24 and the relative k_E's of Table I). In addition, Bazelyansky et al.[39] have estimated a binding rate constant k_1 of (2–3) × 10^7 M^{-1} s^{-1} for AChE-catalyzed hydrolysis of 3,3-dimethylbutyl thioacetate. This value is an order of magnitude larger than k_E of PMPF, the most reactive substrate of Table I.

Equation 8 is a useful expression because it can be used to rationalize the low pK_a's determined from pH–rate profiles (cf. Figure 1 and Table I), the nonlinear proton inventories of Figure 2, and the nonlinear Eyring plots, such as that in Figure 3 for PMPF. For example, at high pH eq 8 becomes

$$k_E = \frac{k_2' k_3'}{k_2' + k_3'} \tag{9}$$

where $k_2' = k_1k_2/k_{-1}$ and $k_3' = k_1k_2k_3/k_{-1}k_{-2}$. Hence, k_E is the harmonic mean of the overall rate constants for conversion of E + S to the transition states of the k_2 and k_3 microscopic steps, respectively. Equations 6 and 7 of Results were derived from eq 9, and eq 7 was used to fit the nonlinear Eyring plot of Figure 3. The bowing upward shape of the plot is consistent with temperature-dependent changes of fractional contributions to rate determination of the serial k_2 and k_3 transition states. The $\Delta G^{\ddagger}$'s calculated from the data of Table II for the serial microscopic steps are in each case about the same, which is consistent with about equal rate determination by the steps. The same general model for acylation rate determination emerges on quantitative analysis of proton inventories for V/K of ONCA,[11] ONA, and ONFA (vida infra). The first of the serial microscopic steps is characterized by small $\Delta H^{\ddagger}$ and large negative $\Delta S^{\ddagger}$. It is tempting to propose that this step involves an AChE conformation change,[40] such as the induced fit that Rosenberry suggests precedes chemical catalysis.[6,8] An induced fit conformation change during acylation is consistent with the known conformational flexibility of the AChE active site.[41,43–45] For the anilide substrates $\Delta S^{\ddagger}_2$ is generally more negative than ΔS = −35 eu estimated by Jencks[46] for formation of the transition state or product of a bimolecular reaction. Moreover, desolvation of the substrate and hydrophobic AChE active site[6] (which contains, among other residues, tyrosine and tryptophan[47]) on formation of ES ought to make a positive contribution to $\Delta S^{\ddagger}_2$.[48] Hence, the component of $\Delta S^{\ddagger}_2$ for conversion of ES to the k_2 transition state should be yet more negative than the values in Table II. These comparisons suggest a more appreciable tightening of the enzyme–substrate assembly in the k_2 transition state than occurs on loss of translational and rotational entropy alone.

Table IV. Virtual Transition-State Contributions and Intrinsic Solvent Isotope Effects and pK_a's for the Acylation Stage of AChE Reactions

substrate	$^{D_2O}k_3$	C	intrinsic $pK_a^{H_2O}$	f_2	f_3
ONFA[a]	2.3 ± 0.3	2.0 ± 0.6	6.1 ± 0.1	0.67 ± 0.24	0.33 ± 0.07
ONA[a]	2.5 ± 0.2	1.4 ± 0.3	6.00 ± 0.09	0.58 ± 0.14	0.42 ± 0.05
ONCA[b]	2.3 ± 0.2	2.0 ± 0.5	6.3 ± 0.1	0.67 ± 0.20	0.33 ± 0.06
PMPF[c]	1.9	≥9	≥6.6	≥0.9	≤0.1

[a] Parameters for ONFA and ONA were calculated by nonlinear-least-squares analyses of proton inventories and pH–rate profiles. See legends of Figures 1 and 2 for experimental conditions. [b] Parameters for ONCA were calculated from the data of Quinn and Swanson.[11] [c] Parameters for PMPF are estimates. See Discussion for elaboration.

The large negative $\Delta S^{\ddagger}_2$ suggests that during acylation catalysis AChE adopts a more rigid conformation that is poised for consequent interaction with the chemical transition state(s). As the substrate becomes poorer (lower k_E) $\Delta H^{\ddagger}_2$ does not vary markedly but $\Delta S^{\ddagger}_2$ is increasingly negative. This trend suggests that the conformational options available to AChE are more restricted for poor substrates. In effect, the enzyme is more tightly poised as the free energy of the chemical transition state(s) (i.e., $\Delta G^{\ddagger}_3$) increases.[49] Hence, $\Delta G^{\ddagger}_2$ increases as $\Delta G^{\ddagger}_3$ increases, so that chemistry never becomes cleanly rate determining as substrate reactivity decreases. The general agreement of the activation parameters for the k_2 step in H_2O and D_2O supports the idea that the same event is being monitored in the isotopic solvents. Similar conclusions are in order for the k_3 step.

Equation 8 can also be used to render a quantitative accounting of the proton inventories of Figure 2. The account that follows is a more detailed presentation of the virtual transition-state model for AChE proton inventories that was communicated previously by Quinn and Swanson.[11] As for the nonlinear Eyring plots discussed above, the k_3 step is assumed to be a chemical catalytic event. Furthermore, this step is assumed to be solvent isotope sensitive (i.e., k_3 involves proton transfer) and pH sensitive (i.e., k_3 depends on the basic form of the active site histidine). If a single proton bridge stabilizes the k_3 transition state,[24,42,50] the requisite Gross–Butler equation is

$$k_{3,n} = k_3^{H_2O}(1 - n + n\Phi_3^T) \tag{10}$$

Substitution of eq 10 into eq 8 gives the following expression for k_E at high pL in mixed isotopic solvents of deuterium atom fraction n and in D_2O (n = 1), respectively.

$$k_{E,n} = \frac{k_1k_2k_3^{H_2O}(1 - n + n\Phi_3^T)}{k_{-1}[k_{-2} + k_3^{H_2O}(1 - n + n\Phi_3^T)]} \tag{11}$$

$$k_E^{D_2O} = \frac{k_1k_2k_3^{H_2O}\Phi_3^T}{k_{-1}[k_{-2} + k_3^{H_2O}\Phi_3^T]} \tag{12}$$

The ratio of eq 11 and 12 is

$$k_{E,n}/k_E^{D_2O} = \frac{(1 - n + n\Phi_3^T)(1 + C\Phi_3^T)}{\Phi_3^T + C\Phi_3^T(1 - n + n\Phi_3^T)} \tag{13}$$

In this equation, $C = k_3^{H_2O}/k_{-2}$ is the commitment to proton transfer catalysis and Φ_3^T is the fractionation factor of the bridging proton of the k_3 transition state. C measures the tendency of ES_2 of Scheme II to continue on to the acylenzyme via the proton transfer transition state vs. reversion of ES_2 to ES_1 via the induced fit transition state. The reciprocal of Φ_3^T is the intrinsic solvent isotope effect for the k_3 step, $^{D_2O}k_3$. When n = 0, eq 13 reduces to eq 14, which gives the relationship of the observed and the intrinsic solvent isotope effects:

(39) Bazelyansky, M.; Robey, E.; Kirsch, J. F. *Biochemistry* **1986**, *25*, 125–130.

(40) Assignment of conformation change to the k_2 step is supported by the effect of decamethonium, an AChE inhibitor that conformationally modulates the enzyme's active site,[41] on the activation energetics for V/K of PMPF hydrolysis. In the presence of saturating decamethonium in H_2O, $\Delta H^{\ddagger}_2$ = 7.0 ± 0.9 kcal/mol, an increase of ~3 kcal/mol (cf. Table II), but $\Delta H^{\ddagger}_3$ remains virtually unchanged at 23.6 ± 0.2 kcal/mol (Barlow, P. N.; Quinn, D. M.; unpublished observations). In addition, when AChE-catalyzed hydrolysis of ONA or ONCA is inhibited by Me_2SO, the proton transfer transition state becomes solely rate determining,[42] since the solvent isotope effect for V/K rises to ~2 and the Eyring plot becomes linear. The $\Delta H^{\ddagger}$ calculated from the Eyring plot of the Me_2SO-inhibited ONCA reaction is the same as $\Delta H^{\ddagger}_3$ of Table II. These observations establish that the microscopic step with the higher $\Delta H^{\ddagger}$ in Table II is indeed the solvent isotope sensitive step.

(41) Berman, H. A.; Becktel, W.; Taylor, P. *Biochemistry* **1981**, *20*, 4803–4810.

(42) Barlow, P. N.; Acheson, S. A.; Swanson, M. L.; Quinn, D. M. *J. Am. Chem. Soc.*, following paper in this issue.

(43) Barnett, P.; Rosenberry, T. L. *J. Biol. Chem.* **1977**, *252*, 7200–7206.

(44) Rosenberry, T. L.; Bernhard, S. A. *Biochemistry* **1972**, *11*, 4308–4321.

(45) Rosenberry, T. L.; Bernhard, S. A. *Biochemistry* **1971**, *10*, 4114–4120.

(46) Jencks, W. P. *Adv. Enzymol. Rel. Areas Mol. Biol.* **1975**, *43*, 219–410.

(47) Majumdar, R.; Balasubramanian, A. S. *Biochemistry* **1984**, *23*, 4088–4093.

(48) Tanford, C. *The Hydrophobic Effect*; Wiley: New York, 1973; pp 16–23.

(49) The k_3 step which we assign to chemical catalysis might itself represent a composite of microscopic events (e.g., the formation and breakdown of tetrahedral intermediates, proton transfers, etc.).

(50) Kovach, I. M.; Larson, M.; Schowen, R. L. *J. Am. Chem. Soc.* **1986**, *108*, 3054–3056.

$$^{D_2O}k_E = \frac{^{D_2O}k_3 + C}{1 + C} \quad (14)$$

Hence, the intrinsic solvent isotope effect is increasingly masked as the commitment to proton transfer catalysis becomes larger (i.e., as the proton transfer transition state becomes less rate determining).[51]

If the virtual transition-state model and its associated host of assumptions are correct, eq 13 should provide satisfactory fits of proton inventories for AChE acylation. Figure 2 displays nonlinear-least-squares fits of ONA and ONFA proton inventories to eq 13; Φ_3^T, C, and $k_E^{D_2O}$ were the adjustable parameters of the least-squares optimization. The good fits support the virtual transition-state model. The commitments to proton transfer catalysis and the intrinsic solvent isotope effects for the k_3 step are given in Table IV, along with values calculated from the data of Quinn and Swanson for ONCA.[11,52] The intrinsic solvent isotope effects for the three anilide substrates agree remarkably well and are similar to solvent isotope effects for deacylation of acetyl–AChE.[8,24,50] The commitments to proton transfer catalysis can be used to calculate the fraction of acylation rate determination by induced fit (f_2) and by the proton transfer step ($f_3 = 1 - f_2$)

$$f_2 = \frac{C}{1 + C} \quad (15)$$

The values of f_2 and f_3 are also given in Table IV.

The commitments can also be used to correct the $pK_a^{H_2O}$ of Table I for the effects of partial rate determination by induced fit (assumed to be pH insensitive), as discussed by Rosenberry[6] and by Quinn and Swanson.[11,53] The corrected values, which are listed in Table IV, are in reasonable agreement with the intrinsic pK_a of 6.3 of the active site histidine. The estimated limits of the parameters for PMPF are also given in Table IV, on the proviso that the proton transfer transition state(s) for PMPF is subject to an intrinsic solvent isotope effect of 1.9.[24,42] The commitments in D_2O, C^{D_2O}, can be calculated by dividing the commitments in H_2O by the corresponding intrinsic solvent isotope effects for k_3. The resulting values are $C^{D_2O} = 0.9 \pm 0.3$ and 0.6 ± 0.1 for ONFA and ONA, respectively. When these commitments are used to correct the observed $pK_a^{D_2O}$'s of Table I (as done above for $pK_a^{H_2O}$), the intrinsic $pK_a^{D_2O} = 6.51 \pm 0.10$ and 6.64 ± 0.06 for ONFA and ONA, respectively. The ΔpK_a's are 0.41 ± 0.22 and 0.64 ± 0.15 for the respective anilides and are within error of the ΔpK_a's of 0.45–0.55 expected for the titration of a weak organic acid. Therefore, the virtual transition-state model for AChE acylation reaction dynamics discussed herein can quantitatively resurrect chemically reasonable pK_a's and solvent isotopic shifts of pK_a's from the phenomenological data.

In summary, we have delineated a detailed virtual transition-state model for the acylation stage of AChE catalysis. In the following paper,[42] we describe experiments which further refine our quantitative accounting of acylation reaction dynamics, and which unmask the acylation proton transfer transition states for AChE-catalyzed anilide hydrolyses.

(51) Equation 14 is equivalent to the expression derived by Northrop for the relationship between observed and intrinsic substrate isotope effects for V/K: Northrop, D. B. In *Isotope Effects on Enzyme-Catalyzed Reactions*; Cleland, W. W., O'Leary, M. H., Northrop, D. B., Eds.; University Park Press: Baltimore, 1977; pp 122–152.

(52) The values in Table IV for ONCA are somewhat different than those of Quinn and Swanson.[11] In the earlier communication, linear-least-squares fits to transforms of eq 4 and 13 were used to calculate Φ_3^T, C, and pK_a.

(53) One can derive the relationship of observed and intrinsic pK_a's by rewriting eq 8 as follows:

$$k_E = \frac{k_3' K_a}{K_a(1 + C) + H^+}$$

In this equation, k_3' and C are as defined in eq 9 and 13 and the accompanying text. Because the intrinsic K_a in the denominator is multiplied by $(1 + C)$, the observed and intrinsic pK_a's are related as follows:

$$pK_a^{int} = pK_a^{obsd} + \log (1 + C)$$